Ab Initio, Density Functional Theory, and Continuum Solvation Model Prediction of the Product Ratio in the S_N2 Reaction of NO_2^- with CH_3CH_2Cl and CH_3CH_2Br in DMSO Solution

Eduard Westphal[†] and Josefredo R. Pliego, Jr*[,‡]

Departamento de Química, Universidade Federal de Santa Catarina, 88040-900, Florianópolis, SC, Brazil, and Departamento de Química, Universidade Federal de Minas Gerais, 31270-901, Belo Horizonte, MG, Brazil

Received: June 21, 2007; In Final Form: July 26, 2007

The reaction pathways for the interaction of the nitrite ion with ethyl chloride and ethyl bromide in DMSO solution were investigated at the *ab initio* level of theory, and the solvent effect was included through the polarizable continuum model. The performance of BLYP, GLYP, XLYP, OLYP, PBE0, B3PW91, B3LYP, and X3LYP density functionals has been tested. For the ethyl bromide case, our best ab initio calculations at the CCSD(T)/aug-cc-pVTZ level predicts product ratio of 73% and 27% for nitroethane and ethyl nitrite, respectively, which can be compared with the experimental values of 67% and 33%. This translates to an error in the relative $\Delta G^{\ddagger}$ of only 0.17 kcal mol^{-1}. No functional is accurate (deviation $<$0.5 kcal mol^{-1}) for predicting relative $\Delta G^{\ddagger}$. The hybrid X3LYP functional presents the best performance with deviation 0.82 kcal mol^{-1}. The present problem should be included in the test set used for the evaluation of new functionals.

Introduction

In the past 20 years, different aspects of S_N2 reactions both in the gas phase and in solution have been theoretically investigated.[1−38] Accurate computation of the energy barrier is an important goal[39] and high level ab initio calculations at coupled-cluster (CCSD(T)) level with aug-cc-pVTZ quality basis set are able to predict gas-phase barrier heights with an error within 1 kcal mol^{-1}.[37,40] For liquid-phase processes, adequate parametrization[41,42] of the polarizable continuum model[43−46] predicts a reliable solvent induced barrier in dipolar aprotic solvents.[1,2] Nevertheless, our ability to predict correctly the relative product ratio of S_N2 reactions involving ambident nucleophiles has not been adequately explored. In this way, this work reports a theoretical prediction of the product outcome of the S_N2 reaction of NO_2^- ion with alkyl halides in dimethyl sulfoxide (DMSO) solution, which produces nitroalkane and alkyl nitrite.

High level wave function based methods are able to provide molecular properties with chemical accuracy,[47] but its application is limited to small systems. On the other hand, density functional theory can be applied for both medium and large systems. Thus, considering the interest of applying theoretical methods for any size system, it is important to know the performance of density functional theory for this kind of problem. Test of current functionals for barrier height calculation has been reported[36,37,48−50] and a lot of papers has been published in past few years aimed at developing accurate functionals for chemical problems, including thermochemical kinetics.[40,51−59] Therefore, this work also analyses the performance of some widely available functionals for predicting relative barrier height investigated in this article.

The nitroalkanes are an important class of organic compounds and there is current interest in more efficient incorporation of the nitro group to organic molecules.[60] Besides the intrinsic interest in nitro compounds, nitroalkanes have acid α-hydrogen adequate to generate carbanions, which are useful species for carbon−carbon bond forming reactions. In recent years, nitroalkanes have been successfully used in organocatalysed reactions.[61−64] A general approach for nitroalkane synthesis is to carry out the reaction of the nitrite ion with an alkyl halide,[65] which proceeds through a bimolecular nucleophilic substitution reaction (S_N2). However, because the nitrite ion is an ambident nucleophile, both the nitroalkane ($R-NO_2$) and the alkyl nitrite ($R-ONO$) are formed. In addition, bimolecular elimination (E2) is a parallel pathway and may lead to reduced S_N2 yields. The four possible reaction pathways are shown at Scheme 1. In the case of elimination, either oxygen (path 3) or nitrogen (path 4) could acts as a base.

Until 1956, it was though that nitrite ion reacted with alkyl halides forming only alkyl nitrite. Kornblum and co-workers[66,67] were able to show that although much alkyl nitrite was formed, the nitroalkane was the main product when the reaction was carried out in dipolar aprotic solvents like dimethylformamide (DMF) or DMSO. No elimination product was reported. More recently, Tishkov et al.[68] have reinvestigated the relative reactivity of the oxygen and nitrogen side of the nitrite ion and have concluded that they have similar reactivity. Despite the importance of this system, no theoretical study of this reaction has been reported to date. Therefore, in this work we have reported the first theoretical study of S_N2 reactions involving the nitrite ion, as well as analyzed the ability of theoretical methods to predict absolute and relative $\Delta G^{\ddagger}$ for competitive ionic reaction in solution.

Theoretical Calculations

We have done four set of calculations. In the first set, full geometry optimization for each species (reactants, transition states and products) was done at the MP2 level using the 6-31+G(d) basis set for all atoms but bromide. In this case, we

* Corresponding author. E-mail: josef@netuno.qui.ufmg.br.
[†] Universidade Federal de Santa Catarina.
[‡] Universidade Federal de Minas Gerais.

10.1021/jp074842x CCC: $37.00
Published on Web 09/20/2007

SCHEME 1

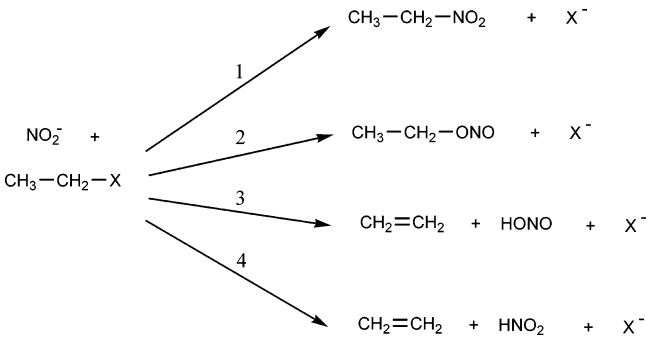

have use the Binning and Curtiss[69] all electron double-ζ valence basis set augmented with sp diffuse (exponent = 0.0376) and d polarization (exponent = 0.389) functions. This basis set for all atoms will be referred as 6-31+G(d). The efficient quadratic approximation method[70] implemented in Gamess program was used in the optimizations. Harmonic frequency calculations were also undertaken at MP2/6-31+G(d) level to determine the gas-phase thermodynamic properties through statistical mechanics calculations.[71,72] We have adopted the standard state of 1 mol L^{-1} for reporting both the gas-phase and solution-phase data. More reliable energies were obtained at MP4 level using the 6-31+G(d) basis set.

The solvent effect was included through the polarizable continuum model (PCM) of Tomasi and co-workers[43−46,73,74] using the Pliego and Riveros parametrization[41,42,75,76] developed for the DMSO solvent. Although there are many theoretical studies about the development of solvation models,[73,77−108] dielectric continuum models remain as the most popular method for including solvent effect. Recent theoretical studies[41,82] have shown that an adequate parametrization of the polarizable continuum model (PCM) for dimethyl sulfoxide (DMSO) solution is able to predict pK_a values of organic acids with an average error of 2 pK_a units. In addition, the activation free energy barriers can be predicted with an error around 2 kcal mol^{-1} in this solvent.[1,2] In these initial calculations, our aim was to analyze the relative importance of the S_N2 and E2 pathways. We have used the BEM routines including correction for the escape charges for the PCM/HF computations and all of these calculations were done with the PC Gamess version[109] of the Gamess United States Quantum Chemistry program.[110]

In the second set of calculations, we have used the gas-phase MP2/6-31+G(d) optimized geometries for running higher level single point calculations. However, in this case only the activation free energy barriers of the S_N2 pathways were investigated. Our aim was to make a reliable prediction of the nitroalkane and the organic nitrite species formed. Therefore, single point energy calculations were done at CCSD(T)/6-31+G(d) level to obtain an effective CCSD(T)/6-311+G(2df,2p) level of theory using MP2/6-311+G(2df,2p) (with 6d and 10f Gaussian orbitals) energies and additivity approximation. Because there are not 6-311G basis set defined for the Br atom, it was used the triple-ζ valence plus polarization (TZVPP) basis set of Ahlrichs and co-workers for this atom.[111] A set of sp diffuse functions was added to this basis set, and we have considered this calculation by using the 6-311+G(2df,2p) quality basis set. The solvent effect was determined at the PCM/B3LYP/6-31+G(d) level using the IEF routines.[112,113] Because the B3LYP method produces a better charge distribution than the Hartree−Fock one, it should lead to improved relative solvation free energy. All of these new set of calculations were done with the Gamess program.

Liquid-phase optimization may have a minor effect on the ionic S_N2 reactions on the primary substrate.[7,114] The effect should be even smaller for reactions in DMSO and involving species with a high charge dispersion like the nitrite ion. A test of the solvent effect on the geometry was done with the TS1 structure of the ethyl bromide reaction. Because Gamess does not have PCM/MP2 optimizations, we have performed B3LYP/6-31+G(d) and PCM/B3LYP/6-31+G(d) optimizations to analyze the change in the geometry.

In the third set of calculations, the effect of more extended aug-cc-pVTZ basis set,[115−117] implemented in the Gamess program, as well as the core electrons excitation was analyzed. In addition, single point PCM/B3LYP/6-311+G(2df,2p) calculations were done to converge the solvent effect.

In the last fourth set of calculations we have analyzed the performance of density functional theory through single point energy calculations on the optimized MP2/6-31+G(d) geometries. Many of the recently developed functionals are not available yet, so we have tested some widely used functionals like BLYP,[118,119] B3LYP,[120] and B3PW91,[121] the GLYP[119,122] functional, and some modern functionals like OLYP,[59,119] XLYP,[55,119,123] PBE0,[124] and X3LYP.[55,119,123] It should be emphasized that Boese et al.[125] have found the Pople basis set adequate for density functional calculations. Thus, we have used the 6-311+G(2df,2p) basis set (6D and 10F) for our DFT computations. All of the DFT calculations were done with the Gamess and PC Gamess programs.

Results and Discussion

$CH_3CH_2Cl + NO_2^-$. In the case of the reaction of the nitrite ion with ethyl chloride, we have investigated all of the reaction pathways presented at Scheme 1 and the full optimized transition state structures are shown at Figure 1. Structure TS1 corresponds to the transition state for nitroalkane formation whereas the reaction leading to the organic nitrite has two transition states, TS2a and TS2b. The gas-phase $\Delta G^{\ddagger}$ for these species, calculated at the MP4/6-31+G(d)//MP2/6-31+G(d) level, are close and around 12.5 kcal mol^{-1} (Table 1). This result indicates a high competition between the nitroalkane and the alkyl nitrite reaction pathways. The solvent effect, obtained at PCM/HF/6-31+G(d) level, is also similar and increases the barrier of TS1 by 14.2 kcal $mol^{-1.}$ In the case of TS2a and TS2b, the solvent effect is slightly greater, increasing the barrier by 15.9 and 15.1 kcal mol^{-1}. The final $\Delta G^{\ddagger}$ for these pathways are in the range 26.9−28.8 kcal mol^{-1} and indicates that both the nitroalkane and the alkyl nitrite are formed in this reaction, the former being the major product.

The usual competing pathway of S_N2 reactions is the E2 process. We have located two transition states related to E2 mechanism. Structure TS3 corresponds to the elimination reaction where the oxygen acts as a base, and in TS4 the nitrogen of the nitrite ion induces the E2 reaction. The corresponding gas-phase $\Delta G^{\ddagger}$ are at least 10 kcal mol^{-1} more positive than the S_N2 pathway. As observed in other systems,[1,32,35] the solvent induced free energy barrier is higher for the E2 process than for the S_N2. As a final result, the $\Delta G^{\ddagger}$ barrier for TS3 and TS4 are 41.5 and 45.4 kcal mol^{-1}, respectively, and the E2 mechanism will not take place at all. Indeed, Table 1 shows that the elimination reactions have positive reaction ΔG values in both the gas phase and DMSO solution. On the other hand, both the nitroalkane and the alkyl nitrite formation have negative reaction free energies.

To make more reliable predictions on the competing S_N2 pathways, a higher level of theory was used. We have done

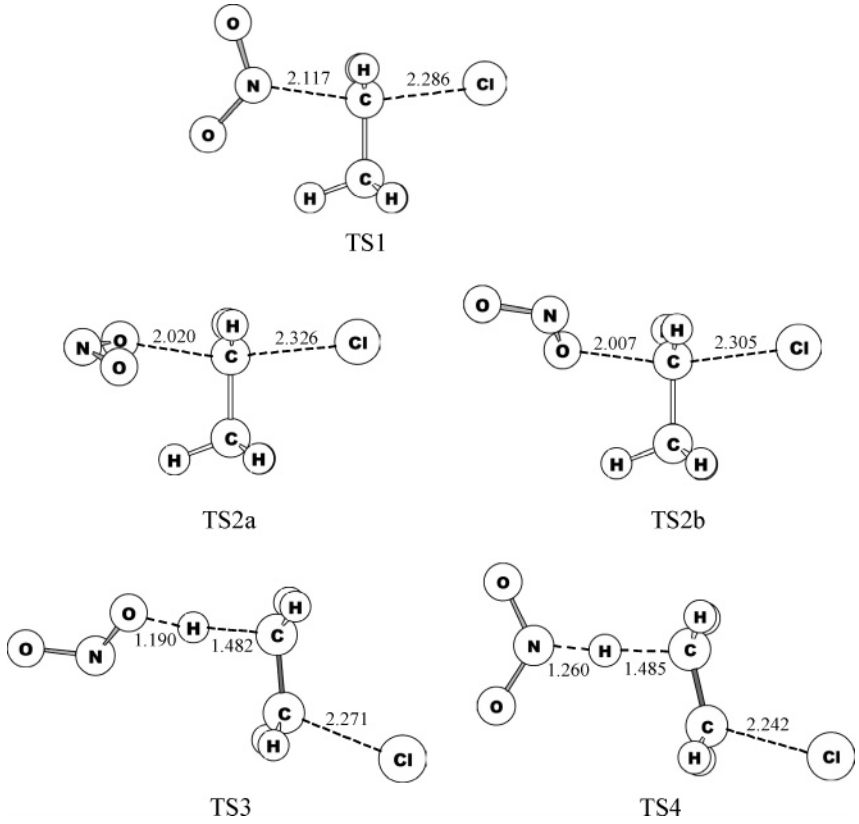

Figure 1. Transition states for the NO_2^- + CH_3CH_2Cl reaction optimized at the MP2/6-31+G(d) level of theory. Bond lenghts in Å.

TABLE 1: Activation and Reaction Properties for the NO_2^- + CH_3CH_2Cl Reaction[a]

	activation				
	TS1	TS2a	TS2b	TS3	TS4
HF/6-31+G(d)	8.15	6.15	7.13	25.53	33.56
MP2/6-31+G(d)	5.86	7.55	7.41	20.42	22.62
MP4/6-31+G(d)	4.11	4.51	4.55	20.21	23.83
$\Delta G_g^{\ddagger}$ [b]	12.65	12.85	12.28	23.66	27.76
$\Delta\Delta G_{solv}^{\ddagger}$ [c]	14.21	15.90	15.06	17.80	17.65
$\Delta G_{sol}^{\ddagger}$ [d]	26.86	28.75	27.34	41.46	45.41
	reaction				
	1	2		3	4
HF/6-31+G(d)	−12.71	−15.06		6.14	17.84
MP2/6-31+G(d)	−10.76	−4.38		20.22	21.95
MP4/6-31+G(d)	−7.90	−5.06		18.96	23.77
ΔG_g	−2.18	−1.26		10.96	17.96
$\Delta\Delta G_{solv}$	−5.87	−2.79		−4.64	−7.68
ΔG_{sol}	−8.05	−4.04		6.32	10.29

[a] Geometry optimization and harmonic frequencies at the MP2/6-31+G(d) level of theory. Standard state of 1 mol/L, 298.15 K. Solvation free energy calculated at the PCM/HF/6-31+G(d) level (DMSO solvent). For TS2a, TS2b, and TS3, the $-RT$ ln(2) factor was included in the activation free energy because there are two isomeric transition states. Units of kcal mol^{-1}. [b] Gas-phase activation free energy. [c] Solvent contribution to the activation free energy. [d] Solution-phase activation free energy, $\Delta G_{sol}^{\ddagger} = \Delta G_g^{\ddagger} + \Delta\Delta G_{solv}^{\ddagger}$.

single point calculations at the CCSD(T)/6-311+G(2df,2p) (additivity approximation) level and included the solvent effect through the PCM/B3LYP/6-31+G(d) method. The results are in Table 2. There are not significant modifications on $\Delta G_{sol}^{\ddagger}$, but the relative contribution of both the gas phase and the solvent for each pathway presents important differences. For example, at the MP4/6-31+G(d) level the TS2b structure is the most stable transition state and it is below the TS1 by 0.37 kcal mol^{-1}

TABLE 2: Activation Properties for the NO_2^- + CH_3CH_2X Reaction[a]

	TS1	TS2a	TS2b
NO_2^- + CH_3CH_2Cl			
MP2/6-31+G(d)	5.87	7.55	7.41
CCSD(T)/6-31+G(d)	4.77	4.53	5.12
MP2/6-311+G(2df,2p)	3.20	5.79	5.54
CCSD(T)/ 6-311+G(2df,2p)[b]	2.11	2.77	3.25
$\Delta G_g^{\ddagger}$ [c]	10.65	11.11	10.99
$\Delta\Delta G_{solv}^{\ddagger}$ [d]	15.70	16.32	15.96
$\Delta G_{sol}^{\ddagger}$ [e]	26.35	27.43	26.95
% product (theoretical)	65	35	
NO_2^- + CH_3CH_2Br			
MP2/6-31+G(d)	−1.05	0.76	0.80
CCSD(T)/6-31+G(d)	−1.77	−1.88	−1.03
MP2/6-311+G(2df,2p)	−0.84	1.50	1.51
CCSD(T)/ 6-11+G(2df,2p)[b]	−1.56	−1.15	−0.32
$\Delta G_g^{\ddagger}$ [c]	7.63	7.36	7.61
$\Delta\Delta G_{solv}^{\ddagger}$ [d]	16.95	17.70	17.17
$\Delta G_{sol}^{\ddagger}$ [e]	24.58	25.06	24.77
% product (theoretical)	46	54	
% product (experimental)[f]	67	33	

[a] Geometry optimization at the MP2/6-31+G(d) level of theory. Standard state of 1 mol/L, 298.15 K. Solvation free energy calculated at the PCM/B3LYP/6-31+G(d) level (DMSO solvent). For TS2a and TS2b, the $-RT$ ln(2) factor was included in the activation free energy barrier because there are two isomeric transition states. Units of kcal mol^{-1}. [b] Obtained by additivity approximation. [c] Gas-phase activation free energy. [d] Solvent contribution to the activation free energy. [e] Solution-phase activation free energy, $\Delta G_{sol}^{\ddagger} = \Delta G_g^{\ddagger} + \Delta\Delta G_{solv}^{\ddagger}$. [f] Reaction of nitrite ion with heptyl bromide in dimethylformamide at room temperature.

($\Delta G_g^{\ddagger}$). At the CCSD(T)/6-311+G(2df,2p) level, this order reverses and the TS1 structure becomes more stable than TS2b by 0.34 kcal mol^{-1}. The solvation contribution remains more positive for both TS2a and TS2b, but the difference in relation to TS1 decreases to 0.72 and 0.26 kcal mol^{-1}. The final $\Delta G^{\ddagger}$

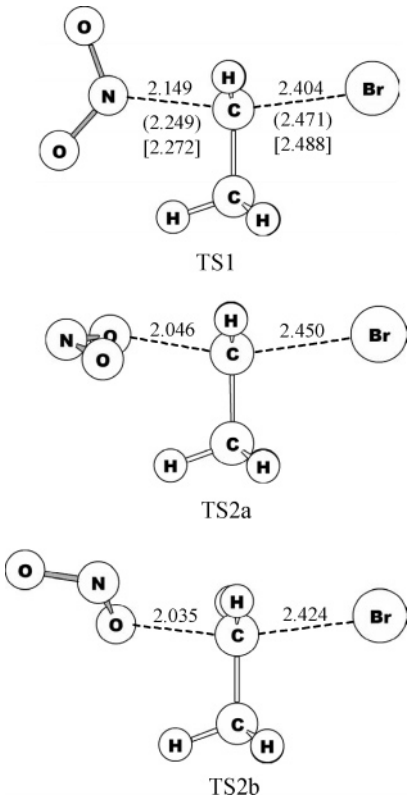

Figure 2. Transition states for the NO_2^- + CH_3CH_2Br reaction optimized at the MP2/6-31+G(d) level of theory. Bond lenghts in Å. For the TS1 structure, geometric parameters obtained at B3LYP/6-31+G(d) (parentheses) and PCM/B3LYP/6-31+G(d) (square brackets) levels were also included.

values are 26.4, 27.4, and 27.0 kcal mol^{-1} for TS1, TS2a, and TS2b, respectively. Therefore, the high competition between the S_N2 pathways remains. These barriers were used to calculate the product ratio through transition state theory in the separable equilibrium solvation approximation.[114] On the basis of this analysis, we have predicted that the nitroethane will be formed in the proportion of 65% against 35% for the alkyl nitrite. There are not experimental data available for alkyl chloride reactions due to relatively slow reaction rates experimentally observed at room temperature, which are consistent with the predicted barriers of 26 kcal mol^{-1}. These reactions are usually performed with alkyl bromides and iodides and in these cases, the nitroalkanes are formed in the proportion around 67% in dipolar aprotic solvents.[66,67]

CH_3CH_2Br + NO_2^-. We have also investigated the ethyl bromide plus nitrite ion reaction at this same high level of theory. Because it was shown that the E2 process for the similar ethyl chloride system has a high free energy barrier, only the S_N2 reactions were investigated. The optimized structures are presented at Figure 2, and they are very similar to the ethyl chloride system. We have also tested the solvent effect on the geometry for the TS1 structure, and the data in Figure 2 show that the effect is minor. The C−Br and C−N bond lengths change by only 0.017 and 0.023 Å, respectively. The effect of MP2 optimizations in relation to B3LYP is more important, and as a consequence, it seems that gas-phase MP2 optimizations are more reliable for this system.

Similarly to ethyl chloride, both the nitroalkane and the alkyl nitrite formation have close gas-phase free energy barriers, corresponding to 7.6, 7.4, and 7.6 kcal mol^{-1} for TS1, TS2a, and TS2b, respectively. This is an important difference in relation to the ethyl chloride system (Table 2), where TS1 is the most stable. However, this gas-phase reactivity order is changed by the solvent effect, which is greater for the TS2a structure, leading to the predicted reactivity TS1 > TS2b > TS2a. The solution-phase free energy barrier becomes 24.6, 25.1, and 24.8 kcal mol^{-1} for TS1, TS2a, and TS2b, respectively. Again, a high competition between the S_N2 pathways is predicted and, as expected, the ethyl bromide is more reactive than the ethyl chloride. In fact, the free energy barriers drop by ~2 kcal mol^{-1}. It is also worth noting that the solvent induced barrier is greater for the ethyl bromide case, meaning that in less polar media, the ethyl bromide reactivity will become even greater than the ethyl chloride.

TABLE 3: Activation Energy (Gas Phase) and Solvent Effect for the NO_2^- + CH_3CH_2Br Reaction Using Different Levels of Theory[a]

	$\Delta E^{\ddagger}$ [b]			
	TS1	TS2a	TS2b	MUE[c]
MP2/6-31+G(d)	−1.05	0.76	0.80	1.38
MP2/6-311+G(2df,2p)	−0.84	1.50	1.51	2.70
MP2/aug-cc-pVTZ	−1.48	1.02	0.96	1.97
MP2(full)/aug-cc-pVTZ	−2.12	1.06	0.84	1.73
CCSD(T)/6-31+G(d)	−1.77	−1.88	−1.03	0.47
CCSD(T)/6-311+G(2df,2p)[d]	−1.56	−1.15	−0.32	0.80
CCSD(T)/aug-cc-pVTZ[d]	−2.20	−1.63	−0.88	0.27
CCSD(T)(full)/aug-cc-pVTZ[d]	**−2.84**	**−1.58**	**−1.00**	
GLYP/6-311+G(2df,2p)	−5.02	−2.47	−1.89	1.32
BLYP/6-311+G(2df,2p)	−7.40	−5.23	−4.48	3.90
XLYP/6-311+G(2df,2p)	−7.61	−5.61	−4.85	4.22
OLYP/6-311+G(2df,2p)	−1.18	2.19	2.22	2.88
PBE0/6-311+G(2df,2p)	−4.76	−2.03	−1.48	0.95
B3PW91/6-311+G(2df,2p)	**−3.92**	**−1.14**	**−0.66**	**0.62**
B3LYP/6-311+G(2df,2p)	−4.60	−2.58	−2.03	1.26
X3LYP/6-311+G(2df,2p)	−5.03	−3.10	−2.52	1.74

	$\Delta\Delta G^{\ddagger}_{solv}$ [e]		
	TS1	TS2a	TS2b
PCM/HF/6-31+G(d)	15.30	17.23	16.31
PCM/B3LYP/6-31+G(d)	16.95	17.70	17.17
PCM/B3LYP/6-311+G(2df,2p)	16.90	17.59	17.14

[a] Units of kcal mol^{-1}. [b] Classical activation barrier in relation to free reactants. [c] Mean unsigned error in relation to CCSD(T)(full)/aug-cc-pVTZ calculation. [d] Obtained by additivity approximation. [e] Solvent effect on the activation free energy.

To determine the product ratio, we can use transition state theory to calculate the rate constant. The results are in Table 2 and indicate that the nitroethane is formed in a proportion of 46%. There are no experimental data for this system, but there are for the related 1-bromoheptane system.[67] In this case, the proportion of nitroalkane is 67%, in good agreement with our theoretical value. It should be remembered that the product ratio is very sensible to the relative $\Delta G^{\ddagger}$, indicating the high quality of our predictions. In addition, the calculations predict that more polar media favor more nitroalkane formation in the cost of decreased reactivity. Recently, Tishkov et al.[68] have studied the reaction of the nitrite ion with $MeOSO_2Me$ in different solvents and observed this effect. For example, in benzene, the nitroalkane product is formed in a ratio of 15% and this value rises to 70% in ethanol.

It would also be interesting to do a comparison with the absolute free energy barrier. Although these data are not available, we can consider the experimental conditions used to carry out the reactions and to make a rough estimate of the $\Delta G^{\ddagger}$. Our estimated experimental $\Delta G^{\ddagger}$ value is ~22.6 kcal mol^{-1} for the reaction of nitrite ion with 1-bromoheptane in DMF,[66] very close to our theoretical value of 24.6 kcal mol^{-1} for the nitroethane formation. In addition, experimental studies

TABLE 4: Activation Free Energy Barrier in DMSO Solution for the $NO_2^- + CH_3CH_2Br$ Reaction Using Different Levels of Theory[a]

	$\Delta G_1^{\ddagger}$	$\Delta G_{2a}^{\ddagger}$	$\Delta G_{2b}^{\ddagger}$	$\Delta G_2^{\ddagger} - \Delta G_1^{\ddagger b}$	deviation
CCSD(T)/6-311+G(2df,2p)	24.58	25.06	24.77	−0.09	−0.51
CCSD(T)/aug-cc-pVTZ	23.94	24.58	24.22	0.02	−0.40
CCSD(T)(full)/aug-cc-pVTZ	**23.31**	**24.63**	**24.10**	**0.59**	**0.17**
GLYP/6-311+G(2df,2p)	21.13	23.73	23.21	1.88	1.46
BLYP/6-311+G(2df,2p)	18.74	20.97	20.61	1.62	1.20
XLYP/6-311+G(2df,2p)	18.53	20.60	20.25	1.46	1.02
OLYP/6-311+G(2df,2p)	24.97	28.40	27.32	2.25	1.83
PBE0/6-311+G(2df,2p)	21.38	24.18	23.61	2.10	1.68
B3PW91/6-311+G(2df,2p)	22.22	25.07	24.44	2.06	1.64
B3LYP/6-311+G(2df,2p)	21.55	23.63	23.07	1.30	0.88
X3LYP/6-311+G(2df,2p)	**21.11**	**23.11**	**22.57**	**1.24**	**0.82**
experimental				**0.42**	

	$\Delta G^{\ddagger}$ (TS1 + TS2a + TS2b)[c]	% nitroalkane
B3PW91/6-311+G(2df,2p)	22.20	94
X3LYP/6-311+G(2df,2p)	21.04	80
CCSD(T)(full)/aug-cc-pVTZ[d]	23.12	73
experimental	(22.6)	67

[a] Units of kcal mol^{-1}. Solvent effect included at the PCM/B3LYP/6-31+G(d) level. Gas-phase geometry and harmonic frequencies obtained at the MP2/6-31+G(d) level of theory. [b] Effective difference of the activation free energy between path 2 and path 1. [c] Observable total activation free energy barrier in DMSO solution. [d] Obtained by additivity approximation.

indicate the lower reactivity of the alkyl chlorides in relation to bromides and iodides and our calculations have predicted that the ethyl chloride is 20 times less reactive than the ethyl bromide.

More Extended Basis Set and the Core Electrons Correlation Effect. In the previous sections, we have analyzed the competition between the S_N2 pathways. Our CCSD(T)/6-311+G(2df,2p) level of theory provides a good estimation of the product ratio, but it would be worth to perform more accurate calculations to see the convergence of the results. Thus, we have performed MP2 calculations with the extended aug-cc-pVTZ basis set in the frozen core approximation and also including the core electrons in the excitation. These calculations were combined with the CCSD(T)/6-31+G(d) one through the additivity approximation to obtain the effective CCSD(T)/aug-cc-pVTZ level of theory. Table 3 presents the results. This more extended basis set produces a small decrease in the barrier, but the relative energies are hardly altered. However, when the core electrons are included, the relative barriers have an important modification and the TS1 structure becomes even more stable. Table 4 shows the final $\Delta G^{\ddagger}$ for each transition state. To do a better comparison of the relative barriers between path 1 and path 2, we have defined the relative activation free energy, through the relation:

$$\Delta G_2^{\ddagger} - \Delta G_1^{\ddagger} = -RT \ln\left[\frac{e^{-\Delta G_{2a}^{\ddagger}/RT} + e^{-\Delta G_{2b}^{\ddagger}/RT}}{e^{-\Delta G_1^{\ddagger}/RT}}\right] \quad (1)$$

The respective experimental value is 0.42 kcal mol^{-1} and our best level of theory (CCSD(T)(full)/aug-cc-pVTZ) predicts a value of 0.59 kcal mol^{-1}, a deviation of only 0.17 kcal mol^{-1} from experimental data, predicting 73% of nitroalkane formation (experimental: 67%). Without the core electrons excitation, the deviation becomes −0.40 kcal mol^{-1}. Considering the contribution of the three transition states to the rate constants, the observed free energy barrier becomes 23.12 kcal mol^{-1}, very close to the experimental value of 22.6 kcal mol^{-1} (Table 4). Therefore, the present high level of theory combined with the continuum solvation model is able to predict accurately the absolute and relative free energy barrier, with an error within 0.5 kcal mol^{-1}.

Convergence of the Solvent Effect. Ionic S_N2 reactions in the liquid phase are processes that present important free energy barriers induced by the solvent. Therefore, much effort has been devoted to the development of solvation models to model this effect and being able to do reliable predictions. Adequate parametrization of the continuum solvation models is critical to achieve this goal. The parametrization of the PCM model used in this work has been shown to be reliable to predict absolute free energy barriers, and the present study points out that it can also be useful to predict relative $\Delta G^{\ddagger}$. Because many chemical reactions in organic chemistry may have parallel pathways leading to different products, this ability is critical to use theoretical methods to estimate the product ratio in chemical reactions of synthetic interest. To test the limit of the PCM model, we have performed more solvation calculations using more extended basis set, the 6-311+G(2df,2p), with the B3LYP functional. Our aim is to compare the electronic density effect on the solvation free energy. Table 3 present three levels of theory. It can be observed that the PCM/B3LYP/6-31+G(d) level is essentially converged when compared with the PCM/B3LYP/6-311+G(2df,2p) level. On the other hand, the PCM/HF/6-31+G(d) level predicts close absolute barrier but overestimates the solvation of the TS1 structure, which would favor this structure for 1.01 kcal mol^{-1} in relation to TS2b, whereas at PCM/B3LYP level, TS1 is more solvated by 0.22 kcal mol^{-1}. Therefore, the PCM/HF calculations are not sufficiently accurate for doing reliable predictions of relative barriers for this system. Previous theoretical analysis of molecular electrostatic potentials and dipole moments of neutral molecules show a remarkable improvement of these properties when going from Hartree−Fock method to hydrid functionals.[126,127]

Performance of Density Functional Theory. The growing popularity of density functional theory and the possibility of its application to larger systems prompted us to investigate how able are the current widely available functionals to predict the product ratio of the nitrite ion plus ethyl bromide reaction. Although there are many recent studies on the performance of density functional theory for predicting absolute energy barriers,[37,40,49,51−54,56,57] the more difficult problem of calculating accurate relative activation barriers of competitive reactions have not received attention. In this work, a total of eight functionals were tested and we have used the CCSD(T)(full)/aug-cc-pVTZ energies as a benchmark. Table 3 shows the classical activation barriers calculated for each transition state using the different functionals, as well as the mean unsigned error (MUE). All the hybrid functionals perform well, with a MUE smaller than 2 kcal mol^{-1}. On the other hand, only the GLYP generalized gradient approximation functional presents a MUE less than 2 kcal mol^{-1}. BLYP, XLYP, and OLYP present a poor performance. The best functional is B3PW91, with a MUE of only 0.62 kcal mol^{-1}.

A more challenging test of the functionals is to predict the relative barriers and the corresponding product ratio. Table 4 presents the performance of the functionals in comparison with experimental data. For this property, the deviation should be smaller than 0.5 kcal mol^{-1}. Otherwise, a large error in the product ratio can result. Table 4 shows that neither functional is able to reach this level of accuracy. X3LYP and B3LYP present the best performance, with a deviation of 0.82 and 0.88 kcal mol^{-1}, whereas the OLYP functional is the worst, with a deviation of 1.83 kcal mol^{-1}. Even the B3PW91 functional, able

to predict an accurate effective free energy barrier, predicts an unacceptable deviation of 1.64 kcal mol^{-1}. Among the GGA functionals, the XLYP present the best performance, with an deviation of 1.02 kcal mol^{-1}. Table 4 presents the overall barrier and the nitroalkane proportion predicted by the B3PW91 and X3LYP functionals. Although the barrier calculated by the B3PW91 is accurate, it predicts a proportion of nitroalkane of 94%, a very high value in relation to experimental one of 67%. For the X3LYP functional, the overall barrier deviates by −1.6 kcal mol^{-1}, and the proportion of the nitroalkane is predicted to be 80%. Therefore, although the X3LYP functional is not very accurate, it presents the best performance for describing S_N2 reactions involving the nitrite ion and alkyl bromides. In this point, it is interesting to notice that in recent reports,[36,37] Bickelhaupt and co-workers has found that the OLYP functional is one of the best functionals for studying S_N2 reactions. Similarly, Baker and Pulay[49] have concluded that the OLYP functional is as good or even better than the popular B3LYP functional. On the basis of our results, it seems that calculation of reliable absolute barrier (error <2 kcal mol^{-1}) may not be enough for determining acceptable relative barriers between competitive reactions (error <0.5 kcal mol^{-1}). In this way, we suggest that the present problem should be used as a test for the development of new functionals.

Conclusion

Ab initio calculations at the CCSD(T)/aug-cc-pVTZ level combined with the polarizable continuum model predict accurate $\Delta G^{\ddagger}$ for the nitrite ion plus ethyl bromide reaction in the DMSO solvent. In addition, the relative free energy barrier between the alkyl nitrite and nitroalkane formation is also very accurately predicted. The solvation free energies calculated at the PCM/B3LYP/6-31+G(d) and PCM/B3LYP/6-311+G(2df,2p) levels are very close. On the other hand, the PCM/HF/6-31+G(d) level is not recommended for predicting relative solvation free energies of competitive transition states. No density functional is accurate (error <0.5 kcal mol^{-1}), and among them, the X3LYP one is the most reliable.

Acknowledgment. We thank the Brazilian Research Council (CNPq) for the support through the Profix program.

References and Notes

(1) Almerindo, G. I.; Pliego, J. R., Jr. *Org. Lett.* **2005**, *7*, 1821.
(2) Tondo, D. W.; Pliego, J. R., Jr. *J. Phys. Chem. A* **2005**, *109*, 507.
(3) Mo, S. J.; Vreven, T.; Mennucci, B.; Morokuma, K.; Tomasi, J. *Theor. Chem. Acc.* **2004**, *111*, 154.
(4) Vayner, G.; Houk, K. N.; Jorgensen, W. L.; Brauman, J. I. *J. Am. Chem. Soc.* **2004**, *126*, 9054.
(5) Fang, Y. R.; Gao, Y.; Ryberg, P.; Eriksson, J.; Kolodziejska-Huben, M.; Dybala-Defratyka, A.; Madhavan, S.; Danielsson, R.; Paneth, P.; Matsson, O.; Westaway, K. C. *Chem. Eur. J.* **2003**, *9*, 2696.
(6) Kahn, K.; Bruice, T. C. *J. Phys. Chem. B* **2003**, *107*, 6876.
(7) Kormos, B. L.; Cramer, C. J. *J. Org. Chem.* **2003**, *68*, 6375.
(8) Mugnai, M.; Cardini, G.; Schettino, V. *J. Phys. Chem. A* **2003**, *107*, 2540.
(9) Sun, L. P.; Song, K. Y.; Hase, W. L.; Sena, M.; Riveros, J. A. *Int. J. Mass Spectrom.* **2003**, *227*, 315.
(10) Laerdahl, J. K.; Uggerud, E. *Int. J. Mass Spectrom.* **2002**, *214*, 277.
(11) Borisov, Y. A.; Arcia, E. E.; Mielke, S. L.; Garrett, B. C.; Dunning, T. H. *J. Phys. Chem. A* **2001**, *105*, 7724.
(12) Gronert, S.; Pratt, L. M.; Mogali, S. *J. Am. Chem. Soc.* **2001**, *123*, 3081.
(13) Michalak, A.; Ziegler, T. *J. Phys. Chem. A* **2001**, *105*, 4333.
(14) Mohamed, A. A.; Jensen, F. *J. Phys. Chem. A* **2001**, *105*, 3259.
(15) Pagliai, M.; Raugei, S.; Cardini, G.; Schettino, V. *Phys. Chem. Chem. Phys.* **2001**, *3*, 2559.
(16) Raugei, S.; Cardini, G.; Schettino, V. *J. Chem. Phys.* **2001**, *114*, 4089.
(17) Re, S.; Morokuma, K. *J. Phys. Chem. A* **2001**, *105*, 7185.
(18) Tachikawa, H. *J. Phys. Chem. A* **2000**, *104*, 497.
(19) Aida, M.; Yamataka, H. *THEOCHEM* **1999**, *462*, 417.
(20) Castejon, H.; Wiberg, K. B. *J. Am. Chem. Soc.* **1999**, *121*, 2139.
(21) Amovilli, C.; Mennucci, B.; Floris, F. M. *J. Phys. Chem. B* **1998**, *102*, 3023.
(22) Yamataka, H.; Aida, M. *Chem. Phys. Lett.* **1998**, *289*, 105.
(23) Chung, D. S.; Kim, C. K.; Lee, B. S.; Lee, I. *J. Phys. Chem. A* **1997**, *101*, 9097.
(24) Streitwieser, A.; Choy, G. S. C.; AbuHasanayn, F. *J. Am. Chem. Soc.* **1997**, *119*, 5013.
(25) Wang, H. B.; Hase, W. L. *J. Am. Chem. Soc.* **1997**, *119*, 3093.
(26) Glukhovtsev, M. N.; Pross, A.; Radom, L. *J. Am. Chem. Soc.* **1996**, *118*, 6273.
(27) Glukhovtsev, M. N.; Pross, A.; Schlegel, H. B.; Bach, R. D.; Radom, L. *J. Am. Chem. Soc.* **1996**, *118*, 11258.
(28) Truong, T. N.; Stefanovich, E. V. *J. Phys. Chem.* **1995**, *99*, 14700.
(29) Hu, W. P.; Truhlar, D. G. *J. Am. Chem. Soc.* **1994**, *116*, 7797.
(30) Evanseck, J. D.; Blake, J. F.; Jorgensen, W. L. *J. Am. Chem. Soc.* **1987**, *109*, 2349.
(31) Chandrasekhar, J.; Smith, S. F.; Jorgensen, W. L. *J. Am. Chem. Soc.* **1985**, *107*, 154.
(32) Pliego, Jr., J. R.; Piló-Veloso, D. *J. Phys. Chem. B* **2007**, *111*, 1752.
(33) Almerindo, G. I.; Pliego, J. R., Jr. *Chem. Phys. Lett.* **2006**, *423*, 459.
(34) Pliego, J. R., Jr. *Org. Biomol. Chem.* **2006**, *4*, 1667.
(35) Pliego, J. R., Jr. *J. Mol. Catal. A* **2005**, *239*, 228.
(36) Swart, M.; Sola, M.; Bickelhaupt, F. M. *J. Comput. Chem.* **2007**, *28*, 1551.
(37) Bento, A. P.; Sola, M.; Bickelhaupt, F. M. *J. Comput. Chem.* **2005**, *26*, 1497.
(38) Halls, M. D.; Raghavachari, K. *Nano Lett.* **2005**, *5*, 1861.
(39) Fernandez-Ramos, A.; Miller, J. A.; Klippenstein, S. J.; Truhlar, D. G. *Chem. Rev.* **2006**, *106*, 4518.
(40) Zheng, J.; Zhao, Y.; Truhlar, D. G. *J. Chem. Theory Comput.* **2007**, *3*, 569.
(41) Almerindo, G. I.; Tondo, D. W.; Pliego, J. R., Jr. *J. Phys. Chem. A* **2004**, *108*, 166.
(42) Pliego, J. R., Jr.; Riveros, J. M. *Chem. Phys. Lett.* **2002**, *355*, 543.
(43) Tomasi, J.; Cammi, R.; Mennucci, B. *Int. J. Quantum Chem.* **1999**, *75*, 783.
(44) Cossi, M.; Barone, V.; Cammi, R.; Tomasi, J. *Chem. Phys. Lett.* **1996**, *255*, 327.
(45) Miertus, S.; Tomasi, J. *Chem. Phys.* **1982**, *65*, 239.
(46) Miertus, S.; Scrocco, E.; Tomasi, J. *Chem. Phys.* **1981**, *55*, 117.
(47) Helgaker, T.; Ruden, T. A.; Jorgensen, P.; Olsen, J.; Klopper, W. *J. Phys. Org. Chem.* **2004**, *17*, 913.
(48) Riley, K. E.; Op't Holt, B. T.; Merz, Jr., K. M. *J. Chem. Theory Comput.* **2007**, *3*, 407.
(49) Baker, J.; Pulay, P. *J. Chem. Phys.* **2002**, *117*, 1441.
(50) Gonzales, J. M.; Cox, R. S.; Brown, S. T.; Allen, W. D.; Schaefer, H. F. *J. Phys. Chem. A* **2001**, *105*, 11327.
(51) Zhao, Y.; Schultz, N. E.; Truhlar, D. G. *J. Chem. Theory Comput.* **2006**, *2*, 364.
(52) Zhao, Y.; Gonzales-Garcia, N.; Truhlar, D. G. *J. Phys. Chem. A* **2005**, *109*, 2012.
(53) Zhao, Y.; Truhlar, D. G. *J. Phys. Chem. A* **2005**, *109*, 5656.
(54) Boese, A. D.; Martin, J. M. L. *J. Chem. Phys.* **2004**, *121*, 3405.
(55) Xu, X.; Goddard, W. A., III. *Proc. Natl. Acad. Sci* **2004**, *101*, 2673.
(56) Zhao, Y.; Truhlar, D. G. *J. Phys. Chem. A.* **2004**, *108*, 6908.
(57) Zhao, Y.; Lynch, B. J.; Truhlar, D. G. *J. Phys. Chem. A* **2004**, *108*, 2715.
(58) Boese, A. D.; Handy, N. C. *J. Chem. Phys.* **2002**, *116*, 9559.
(59) Handy, N. C.; Cohen, A. J. *Mol. Phys.* **2001**, *99*, 403.
(60) Ballini, R.; Barboni, L.; Giarlo, G. *J. Org. Chem.* **2004**, *69*, 6907.
(61) Li, H.; Wang, B.; Deng, L. *J. Am. Chem. Soc.* **2006**, *128*, 732.
(62) Sohtome, Y.; Takemura, N.; Iguchi, T.; Hashimoto, Y.; Nagasawa, K. *Synlett* **2006**, 144.
(63) Marcelli, T.; van der Haas, R. N. S.; van Maarseveen, J. H.; Hiemstra, H. *Synlett* **2005**, 2817.
(64) Prieto, A.; Halland, N.; Jorgensen, K. A. *Org. Lett.* **2005**, *7*, 3897.
(65) Smith, M. B.; March, J. *March's Advanced Organic Chemistry*; John Wiley & Sons: New York, 2001.
(66) Kornblum, N.; Powers, J. W. *J. Org. Chem.* **1957**, *22*, 455.
(67) Kornblum, N.; Larson, H. O.; Blackwood, R. K.; Mooberry, D. D.; Oliveto, E. P.; Graham, G. E. *J. Am. Chem. Soc.* **1956**, *78*, 1497.
(68) Tishkov, A. A.; Schmidhammer, U.; Roth, S.; Riedle, E.; Mayr, H. *Angew. Chem., Int. Ed.* **2005**, *44*, 4623.
(69) Binning, R. C.; Curtiss, L. A. *J. Comput. Chem.* **1990**, *11*, 1206.
(70) Culot, P.; Dive, G.; Nguyen, V. H.; Ghuysen, J. M. *Theor. Chim. Acta* **1992**, *82*, 189.
(71) McQuarrie, D. A. *Statistical Mechanics*; University Science Books: Sausalito, CA, 2000.

(72) Hill, T. L. *An Introduction to Statistical Thermodynamics*; Addison-Wesley: Reading, MA, 1960.
(73) Tomasi, J.; Mennucci, B.; Cammi, R. *Chem. Rev.* **2005**, *105*, 2999.
(74) Tomasi, J.; Persico, M. *Chem. Rev.* **1994**, *94*, 2027.
(75) Pliego, Jr., J. R.; Riveros, J. M. *Phys. Chem. Chem. Phys.* **2002**, *4*, 1622.
(76) Westphal, E.; Pliego, J. R., Jr. *J. Chem. Phys.* **2005**, *123*, 074508.
(77) Boes, E. S.; Livotto, P. R.; Stassen, H. *Chem. Phys.* **2006**, *331*, 142.
(78) Curutchet, C.; Orozco, M.; Luque, F. J.; Mennucci, B.; Tomasi, J. *J. Comp. Chem.* **2006**, *27*, 1769.
(79) Curutchet, C.; Bidon-Chanal, A.; Soteras, I.; Orozco, M.; Luque, F. J. *J. Phys. Chem. B* **2005**, *109*, 3565.
(80) Soteras, I.; Curutchet, C.; Bidon-Chanal, A.; Orozco, M.; Luque, F. J. *THEOCHEM* **2005**, *727*, 29.
(81) Takano, Y.; Houk, K. N. *J. Chem. Theory Comput.* **2005**, *1*, 70.
(82) Fu, Y.; Liu, L.; Li, R.; Liu, R.; Guo, Q. *J. Am. Chem. Soc.* **2004**, *126*, 814.
(83) Li, H.; Jensen, J. H. *J. Comput. Chem.* **2004**, *25*, 1449.
(84) Asthagiri, D.; Pratt, L. R.; Ashbaugh, H. S. *J. Chem. Phys.* **2003**, *119*, 2702.
(85) Curutchet, C.; Cramer, C. J.; Truhlar, D. G.; Ruiz-Lopez, M. F.; Rinaldi, D.; Orozco, M.; Luque, F. J. *J. Comput. Chem.* **2003**, *24*, 284.
(86) Grossfield, A.; Ren, P. Y.; Ponder, J. W. *J. Am. Chem. Soc.* **2003**, *125*, 15671.
(87) Hofinger, S.; Zerbetto, F. *Chem. Eur. J.* **2003**, *9*, 566.
(88) Levy, R. M.; Zhang, L. Y.; Gallicchio, E.; Felts, A. K. *J. Am. Chem. Soc.* **2003**, *125*, 9523.
(89) Luque, F. J.; Curutchet, C.; Munoz-Muriedas, J.; Bidon-Chanal, A.; Soteras, I.; Morreale, A.; Gelpi, J. L.; Orozco, M. *Phys. Chem. Chem. Phys.* **2003**, *5*, 3827.
(90) Chipman, D. M. *J. Chem. Phys.* **2002**, *116*, 10129.
(91) Cossi, M.; Scalmani, G.; Rega, N.; Barone, V. *J. Chem. Phys.* **2002**, *117*, 43.
(92) Hou, T. J.; Qiao, X. B.; Zhang, W.; Xu, X. J. *J. Phys. Chem. B* **2002**, *106*, 11295.
(93) Tomasi, J.; Cammi, R.; Mennucci, B.; Cappeli, C.; Corni, S. *Phys. Chem. Chem. Phys.* **2002**, *4*, 5697.
(94) Tse, J. S. *Annu. Rev. Phys. Chem.* **2002**, *53*, 249.
(95) Curutchet, C.; Orozco, M.; Luque, F. J. *J. Comput. Chem.* **2001**, *22*, 1180.
(96) Grant, J. A.; Pickup, B. T.; Nicholls, A. *J. Comput. Chem.* **2001**, *22*, 608.
(97) Cheng, A.; Best, S. A.; Merz, Jr., K. M.; Reynolds, C. H. *J. Mol. Graphics Modell.* **2000**, *18*, 273.
(98) Colominas, C.; Luque, F. J.; Teixido, J.; Orozco, M. *Chem. Phys.* **1999**, *240*, 253.
(99) Li, J.; Zhu, T.; Hawkins, G. D.; Winget, P.; Liotard, D. A.; Cramer, C. J.; Truhlar, D. G. *Theor. Chem. Acc.* **1999**, *103*, 9.
(100) Pliego, J. R., Jr.; Riveros, J. M. *J. Phys. Chem. A* **2002**, *106*, 7434.
(101) Pliego, J. R., Jr.; Riveros, J. M. *J. Phys. Chem. A* **2001**, *105*, 7241.
(102) Cramer, C. J.; Truhlar, D. G. *Chem. Rev.* **1999**, *99*, 2161.
(103) Li, J.; Hawkins, G. D.; Cramer, C. J.; Truhlar, D. G. *Chem. Phys. Lett.* **1998**, *288*, 293.
(104) Li, J.; Zhu, T.; Cramer, C. J.; Truhlar, D. G. *J. Phys. Chem.* **1998**, *102*, 1820.
(105) Bandyopadhyay, P.; Gordon, M. S. *J. Chem. Phys.* **2000**, *113*, 1104.
(106) Chen, W.; Gordon, M. S. *J. Chem. Phys.* **1996**, *105*, 11081.
(107) Day, P. N.; Jensen, J. H.; Gordon, M. S.; Webb, S. P.; Stevens, W. J.; Krauss, M.; Garmer, D.; Basch, H.; Cohen, D. *J. Chem. Phys.* **1996**, *105*, 1968.
(108) Boes, E. S.; de Andrade, J.; Stassen, H.; Goncalves, P. F. B. *Chem. Phys. Lett.* **2007**, *436*, 362.
(109) Granovsky, A. A. www http://classic.chem.msu.su/gran/gamess/index.html, 2003.
(110) Schmidt, M. W.; Baldridge, K. K.; Boatz, J. A.; Elbert, S. T.; Gordon, M. S.; Jensen, J. H.; Koseki, S.; Matsunaga, N.; Nguyen, K. A.; Su, S.; Windus, T. L.; Dupuis, M.; Montgomery, Jr., J. A. *J. Comput. Chem.* **1993**, *14*, 1347.
(111) Weigend, F.; Haeser, M.; Patzelt, H.; Ahlrichs, R. *Chem. Phys. Lett.* **1998**, *294*, 143.
(112) Cances, E.; Mennucci, B.; Tomasi, J. *J. Chem. Phys.* **1997**, *107*, 3032.
(113) Mennucci, B.; Cances, E.; Tomasi, J. *J. Phys. Chem. B* **1997**, *101*, 10506.
(114) Chuang, Y. Y.; Cramer, C. J.; Truhlar, D. G. *Int. J. Quantum Chem.* **1998**, *70*, 887.
(115) Dunning, T. H., Jr. *J. Chem. Phys.* **1989**, *90*, 1007.
(116) Kendall, R. A.; Dunning, T. H.; Harrison, R. J. *J. Chem. Phys.* **1992**, *96*, 6796.
(117) Woon, D. E.; Dunning, T. H. *J. Chem. Phys.* **1993**, *98*, 1358.
(118) Becke, A. D. *Phys. Rev. A* **1988**, *38*, 3098.
(119) Lee, C.; Yang, W.; Parr, R. G. *Phys. Rev. B* **1988**, *37*, 785.
(120) Stephens, P. J.; Devlin, F. J.; Chabalowski, C. F.; Frisch, M. J. *J. Phys. Chem.* **1994**, *98*, 11623.
(121) Becke, A. D. *J. Chem. Phys.* **1993**, *98*, 5648.
(122) Gill, P. M. W. *Mol. Phys.* **1996**, *89*, 433.
(123) Su, J. T.; Xu, X.; Goddard, W. A., III. *J. Phys. Chem. A* **2004**, *108*, 10518.
(124) Adamo, C.; Cossi, M.; Barone, V. *THEOCHEM* **1999**, *493*, 145.
(125) Boese, A. D.; Martin, J. M. L.; Handy, N. C. *J. Chem. Phys.* **2003**, *119*, 3005.
(126) Soliva, R.; Luque, F. J.; Orozco, M. *Theor. Chem. Acc.* **1997**, *98*, 42.
(127) Soliva, R.; Orozco, M.; Luque, F. J. *J. Comput. Chem.* **1997**, *18*, 980.